Acta Crystallographica Section D
Biological Crystallography
ISSN 0907-4449

Structure of ATP-dependent phosphoenolpyruvate carboxykinase from *Thermus thermophilus* HB8 showing the structural basis of induced fit and thermostability

Michihiro Sugahara, Noriyasu Ohshima, Yoko Ukita, Mitsuaki Sugahara and Naoki Kunishima*

Advanced Protein Crystallography Research Group, RIKEN Harima Institute at SPring-8, 1-1-1 Kouto, Mikazuki-cho, Sayo-gun, Hyogo 679-5148, Japan

Correspondence e-mail: kunisima@spring8.or.jp

Received 31 May 2005
Accepted 19 August 2005

PDB References: phosphoenolpyruvate carboxykinase, unliganded form, 1j3b, r1j3bsf; ATP-liganded form, 1xkv, r1xkvsf.

In order to understand the induced fit and the thermostabilization mechanisms of ATP-dependent phosphoenolpyruvate carboxykinase, the crystal structure of the enzyme from the extreme thermophile *Thermus thermophilus* HB8 (*Tt*PEPCK) was determined and compared with those of orthologues of known structure from two mesophilic organisms. The protomer structures in these orthologues, which exhibit open/closed interdomain conformations, are similar. Isomorphous crystals of unliganded and ATP-bound *Tt*PEPCK were obtained. The asymmetric units of both crystal forms contain two protomers *A* and *B* with closed and open conformations, respectively. ATP was only observed in the interdomain cleft of the closed protomer, suggesting that the induced fit of *Tt*PEPCK agrees with the so-called 'conformational selection' mechanism where ligand binding is not essential for domain closure although its binding leads to the stabilization of the closed state. A bound calcium observed in the N-terminal domain of *Tt*PEPCK probably contributes to the thermal stability. A combination of hydrophobic effects, ion pairs and entropic effects might also contribute to the thermostability of *Tt*PEPCK.

1. Introduction

Phosphoenolpyruvate carboxykinases (ATP-dependent PEPCKs, EC 4.1.1.49; GTP-dependent PEPCKs, EC 4.1.1.32) are widely distributed enzymes found in all known groups of organisms (Utter & Kolenbrander, 1972). They catalyze the reversible decarboxylation and phosphorylation of oxaloacetate to yield phosphoenolpyruvate and carbon dioxide, using ATP or GTP for the phosphoryl transfer with a strict requirement for magnesium ion. In humans and other mammals, PEPCK plays a central role as a regulatory enzyme in gluconeogenesis and is important for stabilizing the blood-glucose level. Gluconeogenic tissues such as kidney and liver convert lactate and other non-carbohydrate molecules to glucose, which in turn is released into the blood. PEPCK is important as a potential drug target in the treatment of non-insulin-dependent diabetes mellitus (NIDDM; Valera *et al.*, 1994). An increase in hepatic gluconeogenesis is believed to be an important factor responsible for fasting hyperglycaemia detected in patients with NIDDM.

The crystal structures of the ATP-dependent PEPCKs from *Escherichia coli* (*Ec*PEPCK; Matte *et al.*, 1996) and *Trypanosoma cruzi* (*Tc*PEPCK; Trapani *et al.*, 2001) have been reported. The crystal structure of *Ec*PEPCK in complex with substrates and metal ions revealed important residues and two metal-ion binding sites in the active site (Tari *et al.*, 1996, 1997) and suggested a plausible reaction mechanism

(Matte *et al.*, 1997, 1998). The polypeptide chain of *Ec*PEPCK folds into two α/β domains (called the N- and C-terminal domains). The substrate-binding and cofactor-binding sites are located in a deep cleft between the two domains. *Ec*PEPCK is known to undergo a conformational transition upon ATP binding. The closed and open forms of *Ec*PEPCK show a difference of 20° in the interdomain orientation (Tari *et al.*, 1996). The active site with bound ATP was shown to adopt the closed form. However, the relationship between ligand binding and domain closure remains obscure.

The change in the orientation upon ligand binding reported in *Ec*PEPCK is an example of so-called 'induced fit' (Anderson *et al.*, 1979). In terms of the relationship between ligand binding and protein activation, induced fit can be classified into two categories: 'classical induced fit', in which the active conformation of the protein appears only after ligand binding (Koshland, 1958), and 'conformational selection', in which the unliganded protein is in equilibrium between the active and the inactive conformations and the ligand-binding selectively stabilizes the active conformation (Berger *et al.*, 1999). This conformational selection mechanism has been proposed in several structures including those of antibodies (Berger *et al.*, 1999) and glutamate receptors (Kunishima *et al.*, 2000). The large interdomain conformational change observed with PEPCK provides an opportunity to examine these two modes of protein activation. Furthermore, a comparison of the induced fit between different PEPCK orthologues may be useful for understanding the general features of the induced fit in this enzyme.

While crystal structures have been determined for PEPCKs from mesophilic organisms, structures of PEPCKs from thermophilic organisms have not yet been reported. Comparative analysis of these structures will provide information on the mechanisms of protein stabilization. Several factors for the thermostabilization of proteins have been proposed based on many crystal structures. These include solvent-exposed surface area in aldehyde ferredoxin oxidoreductase (Chan *et al.*, 1995), packing density in glutamate dehydrogenase and citrate synthase (Britton *et al.*, 1995; Russell *et al.*, 1994), core hydrophobicity in creatinase (Schumann *et al.*, 1993), the length of surface loops in citrate synthase (Russell *et al.*, 1994), hydrogen bonds in D-glyceraldehyde-3-phosphate dehydrogenase (Tanner *et al.*, 1996) and ion pairs in indole-3-glycerol phosphate synthase, holo-glyceraldehyde-3-phosphate dehydrogenase and glutamate dehydrogenase (Hennig *et al.*, 1995; Korndorfer *et al.*, 1995; Yip *et al.*, 1995). These reports indicate that the elucidation of thermostabilization factors for each specific protein requires individual three-dimensional structural comparison between orthologues with different thermostabilities.

In this work, the crystal structure of PEPCK from the extreme thermophile *Thermus thermophilus* HB8, which has an optimum growth temperature of 348 K (*Tt*PEPCK), has been determined. This is the first structure of this enzyme from a thermophilic organism. A three-dimensional structural comparison of three PEPCK orthologues including the mesophilic *Ec*PEPCK and *Tc*PEPCK provides insight into the induced fit and the thermostabilization mechanisms of PEPCK.

2. Materials and methods

2.1. Sample preparation

The expression plasmid pET-11a carrying a gene encoding *Tt*PEPCK (residues 1–529) from the *T. thermophilus* HB8 genome (Yokoyama *et al.*, 2000) was prepared by RIKEN Structurome Group. *E. coli* BL21 (DE3) cells were transformed with the expression plasmid and grown at 310 K in Luria–Bertani medium containing 50 μg ml^{-1} ampicillin for 20 h. The cells were harvested by centrifugation at 4500*g* for 5 min, suspended in 20 m*M* Tris–HCl pH 8.0 (buffer *A*) containing 0.5 *M* NaCl and 5 m*M* 2-mercaptoethanol, disrupted by sonication and heated at 343 K for 10 min. After the heat treatment, cell debris and denatured proteins were removed by centrifugation (20 000*g*, 30 min) and the supernatant was used as the crude extract for purification. The crude extract was desalted using a HiPrep 26/10 desalting column (Amersham Biosciences) and applied onto a SuperQ Toyopearl 650M column (Tosoh) equilibrated with buffer *A*. Proteins were eluted with a linear gradient of 0–0.3 *M* NaCl. After replacement with buffer *A*, the fraction containing *Tt*PEPCK was subjected to a Resource Q column (Amersham Biosciences) equilibrated with buffer *A* and eluted with a linear gradient of 0–0.3 *M* NaCl in buffer *A*. After buffer replacement with 10 m*M* phosphate–NaOH pH 7.0, the fraction containing *Tt*PEPCK was applied onto a Bio-Scale CHT-20-I column (Bio-Rad) equilibrated with the same buffer. Proteins were eluted with a linear gradient of 10–200 m*M* phosphate–NaOH pH 7.0. The fraction containing *Tt*PEPCK was concentrated by ultrafiltration (Vivaspin, 30 kDa cutoff, Vivascience) and loaded onto a HiLoad 16/60 Superdex 200pg column (Amersham Biosciences) equilibrated with buffer *A* containing 0.2 *M* NaCl. The homogeneity and identity of the purified sample were assessed by SDS–PAGE and N-terminal sequence analysis. Finally, the purified *Tt*PEPCK was concentrated to 13.3 mg ml^{-1} and stored at 203 K.

The oligomeric state of purified *Tt*PEPCK was examined by a dynamic light-scattering experiment using a DynaPro MS/X (Protein Solutions) instrument at a protein concentration of 1.0 mg ml^{-1} in 0.2 *M* NaCl and 20 m*M* Tris–HCl pH 8.0. Several measurements were taken at 291 K and analyzed using the program *DYNAMICS* v.3.30 (Protein Solutions). A bimodal analysis revealed an estimated molecular weight of 138 kDa, which is consistent with a homodimeric state in solution.

2.2. Enzymatic analysis

Prior to assays, all enzyme solutions were dialyzed against 10 m*M* HEPES–NaOH buffer pH 7.4 containing 1 m*M* EDTA. After dialysis, the enzyme solutions were further dialyzed against the same buffer without EDTA. The PEPCK reaction forms phosphoenolpyruvate from ATP and oxalo-

acetate. The reaction rate was spectrophotometrically measured by a coupling assay using pyruvate kinase and lactate dehydrogenase at 308 K (Yoshizaki & Imahori, 1979). The reaction mixture consisted of 50 m*M* HEPES–NaOH pH 7.4, 1 m*M* ATP, 1 m*M* oxaloacetate, 1 m*M* ADP, 5 m*M* $MgCl_2$, 0.3 m*M* NADH, 1 unit of pyruvate kinase, 1.5 units of lactate dehydrogenase and various concentrations of $CaCl_2$ (0–0.50 m*M*). The rate of NADH oxidation, which is equivalent to the rate of PEPCK formation, was determined by monitoring the decrease in absorbance at 340 nm using a molecular extinction coefficient of 6200 M^{-1} cm^{-1} for NADH. The concentration of *Tt*PEPCK was estimated from the absorbance at 280 nm, assuming $E^{1\%}_{1\,cm} = 13.5$ from the modified absorption coefficient based on the amino-acid composition (Pace *et al.*, 1995). Specific activity and standard deviation were estimated three times and were found to be 0.13 ± 0.02 µmol min^{-1} mg^{-1} without $CaCl_2$, 0.15 ± 0.03 µmol min^{-1} mg^{-1} with 0.1 m*M* $CaCl_2$ and 0.15 ± 0.02 µmol min^{-1} mg^{-1} with 0.5 m*M* $CaCl_2$.

2.3. Differential scanning calorimetry (DSC)

DSC experiments were performed with a MicroCal VP-DSC capillary cell microcalorimeter. All enzyme solutions were dialyzed against 100 m*M* HEPES–NaOH pH 7.4 and the buffer was used as a reference. The concentration of *Tt*PEPCK was 4.3 µ*M*. Buffer scans were subtracted from *Tt*PEPCK scans. DSC data were analyzed using the *Origin* software supplied with the instrument (MicroCal Inc.). Molar excess heat capacities (C_p) were obtained by normalizing with the *Tt*PEPCK concentration and the volume of the calorimeter cell. Apparent denaturation temperatures (T_m) values were determined as the temperature showing maximum C_p.

2.4. Crystallization, data collection and structure determination

Diffraction-quality crystals of *Tt*PEPCK were obtained using the oil-microbatch method implemented in the TERA automatic crystallization system (Sugahara & Miyano, 2002), in which 0.5 µl of 13.3 mg ml^{-1} protein solution was mixed with 0.5 µl precipitant solution composed of 1.3 *M* potassium phosphate, 0.91 *M* sodium phosphate pH 6.3 for the unliganded form and 0.91 *M* potassium phosphate, 1.3 *M* sodium phosphate pH 6.8, 5 m*M* ATP for the ATP-liganded form. Crystals grew at 291 K over 4–6 d. The orthorhombic crystals grew to typical maximum dimensions of 0.2 × 0.1 × 0.07 mm. The crystals were flash-frozen with a cryosolvent consisting of 30%(*w*/*v*) glycerol and artificial precipitant solution.

The unliganded form crystals belonged to space group $P2_12_12_1$, with unit-cell parameters a = 64.70, b = 129.91, c = 173.39 Å, and contained two chains of *Tt*PEPCK in the asymmetric unit. Diffraction data were collected using an ADSC Quantum4 CCD detector at beamline BL38B1 of SPring-8, Japan. The ATP-liganded crystals were nearly isomorphous to the unliganded crystals; they belonged to space group $P2_12_12_1$, with unit-cell parameters a = 64.07, b = 130.55, c = 174.20 Å. Diffraction data were collected using a Rigaku R-AXIS V imaging-plate detector at beamline BL26B1 of SPring-8, Japan. All data were processed with the program *HKL*2000 (Otwinowski & Minor, 1997).

Table 1
Data-collection and refinement statistics.

Values in parentheses are for the outermost shell.

	Unliganded form	ATP-liganded form
Data collection		
Wavelength (Å)	1.0000	1.0000
Resolution range (Å)	50–2.0 (2.07–2.00)	40–2.2 (2.28–2.20)
No. of reflections measured	726185	52396
No. of unique reflections	99163	75829
R_{merge}† (%)	7.4 (71.3)	8.3 (54.2)
Completeness (%)	99.9 (100.0)	100.0 (100.0)
$I/\sigma(I)$	8.0 (4.2)	9.3 (4.1)
Refinement statistics		
Resolution range (Å)	40–2.0 (2.07–2.00)	40–2.2 (2.28–2.20)
Total No. of reflections	98955	75748
R value	0.21 (0.29)	0.19 (0.24)
R_{free} value (5% reflections)	0.23 (0.31)	0.22 (0.27)
Average B factor (Å^2)	36.6	28.9
R.m.s. deviations from ideal geometry		
Bond distance (Å)	0.01	0.01
Bond angles (°)	1.4	1.5
Ramanchandran plot, residues in (%)		
Most favoured regions	89.8	89.7
Allowed regions	9.9	10.1
Generously allowed	0.3	0.2
Disallowed	0.0	0.0

† $R_{merge} = \sum_i \sum_j |\langle I\rangle - I_{ij}| / \sum_i \sum_j I_{ij}$, where $\langle I_i\rangle$ is the mean intensity of the ith unique reflection and I_{ij} is the intensity of its jth observation.

Positioning of the two PEPCK molecules in the asymmetric unit was first carried out using the molecular-replacement method as implemented in the program *AMoRe* (Navaza, 1994) based on the *Ec*PEPCK crystal structure deposited in the Protein Data Bank (PDB code 1oen). Manual model revision was performed using the *QUANTA*2000 software (Accelrys Inc.). The program *CNS* (Brünger *et al.*, 1998) was used for structure refinement and electron-density map calculation. Each cycle of refinement with bulk-solvent and overall anisotropic *B*-factor corrections consisted of rigid-body refinement, simulated annealing incorporating the slow-cool protocol, positional refinement and *B*-factor refinement (individual or group). Several cycles of model revision and refinement yielded the final model. The refined model of the unliganded form comprises two chains (*A* and *B*) of *Tt*PEPCK, nine phosphate ions, two calcium ions, two glycerol molecules and 714 water molecules in the asymmetric unit. Of the expected 529 amino-acid residues per protomer, residue 1 from both chains, residues 141–146 from chain *A*, residue 529 from chain *B* and residues 377–385 from both chains are assumed to be disordered and are excluded from the coordinate set. All the disordered residues are located far from the active site on the molecular surface of the protein. Examination using *PROCHECK* (Laskowski *et al.*, 1993) revealed excellent stereochemistry for all except 0.3% of the residues, which were in generously allowed regions of Ramachandran plot. The structure of the ATP-liganded form was isomorphous to that of the unliganded form and was determined by difference Fourier analysis using the unliganded model. The

Table 2
The contribution of intraprotomer interactions to the thermal stability of PEPCKs.

ΔG and $\Delta\Delta G$ values upon denaturation are shown in kJ mol^{-1}.

			Nonpolar interactions				Polar interactions						
			Denature ΔASA (Å^2)				Hydrogen bonds			Ion pairs		Entropy	
Enzyme	No. of residue	ASA (Å^2)	C/S	N/O	ΔG	$\Delta\Delta G$	No.	ΔG	$\Delta\Delta G$	No. < 3.4 Å	No. < 5.0 Å	ΔG ($-T\Delta S$)†	$\Delta\Delta G$
*Tt*PEPCK	529	20191	35699	16232	6143	0	823	6996	0	46	82	−487	0
*Tc*PEPCK‡	524	19936	35430	16784	6088	−55	839	7132	136	36	86	−543	−55
*Ec*PEPCK§	541	19938	34994	17048	6007	−136	799	6792	−204	25	57	−583	−96

† Values of entropy are calculated at 310.15 K. ‡ Model used was 1ii2. § Model used was 1oen.

refinement was performed in the same way as that of the unliganded form. The final model of the ATP-liganded form is basically similar to that of the unliganded form, except for the presence of an ATP molecule in chain *A*. Statistics of the data collection and refinement are shown in Table 1. Figs. 1, 3 and 4 were drawn using *QUANTA*2000.

2.5. Semi-empirical evaluation of protein stability

In order to estimate the energy of intraprotomer interaction quantitatively, we calculated three thermo-parameters. Firstly, the value of dissociation ΔG for hydrophobic interaction was calculated based on the accessible surface area (ASA) of nonpolar and polar atoms (Funahashi *et al.*, 1999; Tanaka *et al.*, 2001) (Table 2). The ASA in the native states were calculated following the procedure of Connolly (1993). The ASA in the denatured states were calculated from the extended structures generated using *Insight II*. Secondly, the ΔG contribution from hydrogen bonds was calculated. The contribution of a hydrogen bond has been estimated to be 8.5 kJ mol^{-1} for a 3 Å bond distance (Takano *et al.*, 1999). Thirdly, the entropic effects upon denaturation were estimated from the amino-acid compositions using the thermodynamic parameters proposed by Oobatake & Ooi (1993).

3. Results and discussion

3.1. Overall structure

The crystal structures of *Tt*PEPCK have been determined in the unliganded and the ATP-liganded form (Table 1). In both forms, the *Tt*PEPCK protomer is subdivided into two α/β domains, which are designated the N- and C-terminal domains (Fig. 1). The overall fold of the *Tt*PEPCK protomer is identical to those of *Ec*PEPCK and *Tc*PEPCK, as expected from their substantial sequence identities (48% with *Ec*PEPCK and 44% with *Tc*PEPCK). The asymmetric unit of each crystal form consists of two protomers. The root-mean-square deviation (r.m.s.d.) for the superposition of corresponding C^{α} atoms was 0.8 Å between the two protomers in *Tt*PEPCK and 1.5–2.5 Å for any pair of protomers between *Tt*PEPCK and *Ec*PEPCK. On the other hand, the r.m.s.d. for the superposition of the corresponding single domains was calculated to be 0.3–0.7 Å for any pair of protomers between the unliganded and the ATP-liganded forms of *Tt*PEPCK, indicating that the change in the relative orientation of N- and C-terminal domains in the *Tt*PEPCK protomer also occurs as observed in *Ec*PEPCK.

The crystallographic asymmetric units of both the unliganded and the ATP-liganded forms contain an apparent homodimer without molecular twofold symmetry (Fig. 1). Dynamic light-scattering experiment also shows a dimeric state for *Tt*PEPCK in solution (see §2). The dimer interface has a substantial buried surface area of 1068 Å^2, which corresponds to 5.3% of the total ASA of the *Tt*PEPCK protomer. However, the dimer interface contains no hydrophobic core and almost no conserved residues. Furthermore, several different types of oligomers have been reported among the PEPCK orthologues: dimers in *T. brucei* (Cymeryng *et al.*, 1995; Hunt & Köhler, 1995; Urbina, 1987), tetramers in *Saccharomyces cerevisiae* (Tortora *et al.*, 1985) and hexamers in *Urochloa panicoides* (Finnegan & Burnell, 1995). In the light of these observations, the oligomeric state of *Tt*PEPCK remains uncertain and needs further investigations.

3.2. Active-site conservation

A deep cleft between the N- and C-terminal domains, which is reported to be the binding site for substrate and cofactor in *Ec*PEPCK, is also observed in *Tt*PEPCK (Fig. 1). The active-site residues of ATP-dependent PEPCK can be classified into four distinct motifs (Matte *et al.*, 1997) (Fig. 2*a*). Kinase-1a, kinase-2, adenine-binding and PEPCK-specific motifs interact with ATP, magnesium cation, adenine and the inhibitor oxalate, respectively. Although the adenine-binding motif is not conserved between ATP-dependent PEPCK and human GTP-dependent PEPCK (Dunten *et al.*, 2002), the kinase-1a, kinase-2 and PEPCK-specific motifs are conserved in both ATP- and GTP-dependent PEPCKs (Matte *et al.*, 1997; Linss *et al.*, 1993; Østerås *et al.*, 1995). Therefore, except for the base-recognition site, the ATP- and the GTP-dependent PEPCK might have similar active-site organizations. Comparison of *Tt*PEPCK and *Ec*PEPCK (PDB code 1ayl) shows that all important amino-acid residues involved in binding substrates and magnesium are conserved (Fig. 3*a*). The nearly identical spatial arrangements of the catalytic residues Arg52, Lys197, His216, Ser234, Asp253 and Arg319 suggest that *Tt*PEPCK and *Ec*PEPCK share the same catalytic mechanism.

3.3. Conformational selection

In order to investigate substrate and cofactor-induced conformational changes in the PEPCK enzymes systematically, *Tt*PEPCK structures were compared with those of *Ec*PEPCK. In a comparison between the open and closed forms in *Ec*PEPCK, the relative rigid-body rearrangement of N- and C-terminal domains was reported to be 20° (Tari *et al.*, 1996). In *Tt*PEPCK, the domain closure is accomplished by small changes in the main-chain torsion angles of the three interdomain hinge regions: a β-turn region consisting of residues 326–341, a helix–turn–β region consisting of residues 192–218 and a β-strand consisting of residues 244–256. Additionally, a local conformational change is observed in the adenine-binding loop containing residues Gly427, Gly430 and Gly436. In order to identify the open/closed interdomain arrangement of *Tt*PEPCK, a superposition of C-terminal domains of chains *A* and *B* was performed (Fig. 3). The r.m.s.d. values between the unliganded and the liganded forms were 0.14 Å for the chain *A* pair and 0.15 Å for the chain *B* pair, indicating that the protomer structures of the respective chains *A* and *B* in the both forms are very similar. The r.m.s.d. values were 1.7 and 2.2 Å between the *Ec*PEPCK closed form and the *Tt*PEPCK–ATP chains *A* and *B*, respectively, and 1.8 and 1.5 Å for the *Ec*PEPCK open form and *Tt*PEPCK–ATP chains *A* and *B*, respectively. From these results, chains *A* and *B* in the *Tt*PEPCK structures can be identified as closed and the open conformers, respectively. In the ATP-liganded form of *Tt*PEPCK, the bound ATP was observed in the interdomain cleft of chain *A* only (Fig. 1), confirming that the closed form has higher affinity for the ligand compared with the open form, which is in agreement with the observation in *Ec*PEPCK. Importantly, chain *A* of the unliganded form of *Tt*PEPCK is in the closed conformation, in spite of the absence of ATP (Fig. 3*b*). Therefore, the ligand is not necessarily required for the domain closure of *Tt*PEPCK.

The change in the orientation upon ligand binding observed in PEPCK is a kind of 'induced fit'. To date, two classes of induced fit are known. In the classical induced fit, the active conformation of the protein only appears after ligand binding (Koshland, 1958). In the recently proposed 'conformational selection', unliganded protein is in equilibrium between the active and the inactive conformations and the ligand binding selectively stabilizes the active conformation (Berger *et al.*, 1999). The closed conformation of *Tt*PEPCK in the unliganded form may indicate the substantial population of the active conformer in solution even in the absence of ligands, thereby supporting conformational selection.

3.4. Calcium-binding site

We found a bound cation in the N-terminal domain of the *Tt*PEPCK structure (Fig. 4). From comparison of its temperature factor with those of neighbouring atoms and from its coordination, this molecule is most likely to be a calcium ion. Since extraneous calcium was not added to the crystallization sample, the calcium binding might be tight and specific. Although the *Tt*PEPCK calcium-binding motif is similar to the well known EF-hand, it comprises a shorter loop 1, an additional loop 2 and an insertion helix between two EF-hand-like helices compared with the canonical EF-hand motif (Figs. 2*b*

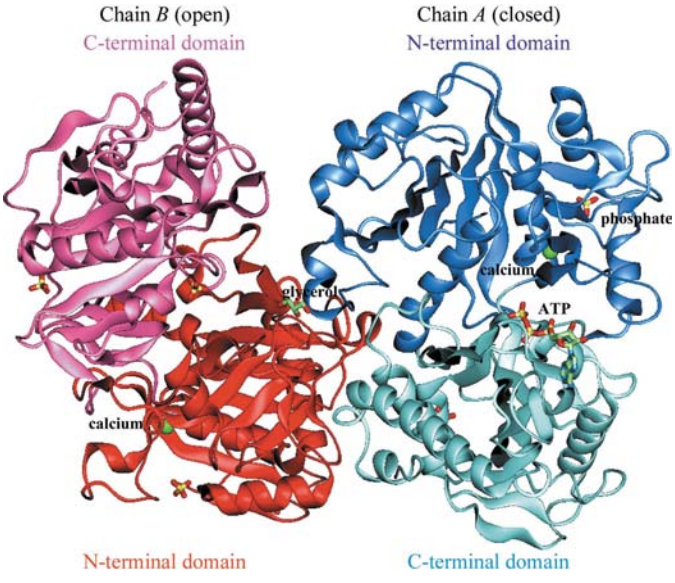

Figure 1
Ribbon diagram of the crystal structure of *Tt*PEPCK. The asymmetric unit of the ATP-liganded form comprising the *A* chain with closed conformation (blue and light blue) and the *B* chain with open conformation (red and pink) is shown. The N- and C-terminal domains are distinguished by dark and light colours, respectively. Bound calcium ions are depicted as green spheres. ATP, phosphate ions and glycerol molecules are depicted as stick models.

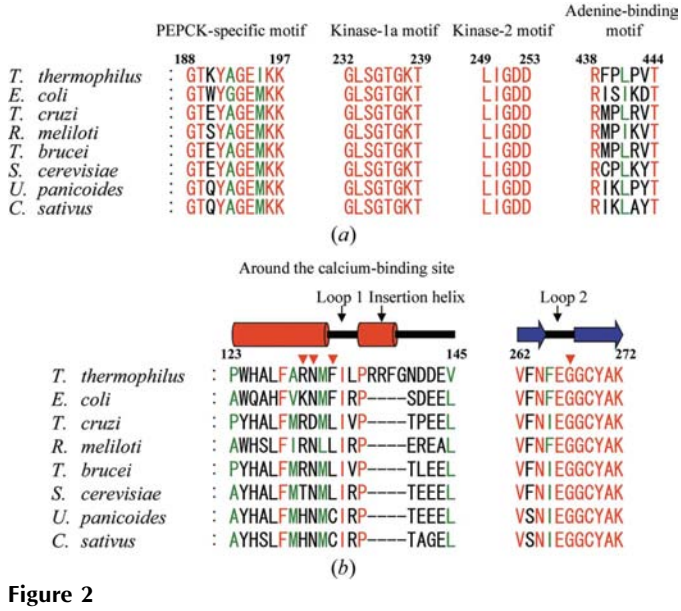

Figure 2
Multiple sequence alignments of ATP-dependent PEPCKs. A multiple sequence alignment of ATP-dependent PEPCK orthologues (from *E. coli*, *T. cruzi*, *Rhizobium meliloti*, *Trypanosoma brucei*, *Saccharomyses cerevisiae*, *Urochloa panicoides* and *Cucumis sativus*) was obtained in order to identify the functionally important residues in PEPCK. (*a*) Selected portions of four active-site regions. Invariant and similar residues are coloured red and green, respectively. (*b*) The residues involved in interaction with the calcium ion (red triangles) with secondary-structure assignment.

and 4). The calcium is recognized by five hydrogen bonds to the main-chain atoms of residues Arg130, Asn131, Phe133 and Gly267 and to a water molecule. In the insertion helix, residues Arg137–Phe139 are not conserved in the PEPCK orthologues.

In *Ec*PEPCK, a bound calcium in the active site has been suggested as an activator of catalysis (Sudom *et al.*, 2003; Delbaere *et al.*, 2004). In the *Tt*PEPCK structure, the active site and the bound calcium in the N-terminal domain are far apart. To examine the activation by calcium in *Tt*PEPCK, the activity of *Tt*PEPCK for oxaloacetate in the presence of 0.1 and 0.5 m*M* concentrations of calcium was measured. The reaction rate was independent of the calcium concentration (see §2), indicating that calcium does not affect the catalysis. These results suggest that the role of calcium in *Tt*PEPCK differs from that in *Ec*PEPCK.

3.5. Thermostability

In order to evaluate the correlation between thermostability and the growth temperature of the source organism, we calculated three thermo-parameters: nonpolar interactions, polar interactions and entropic effects. The hydrophobic interactions in the interior of a protein are an important stabilizing factor (Kauzmann, 1959). The ΔG value arising from hydrophobic interactions in *Tt*PEPCK is greater than those of *Ec*PEPCK and *Tc*PEPCK (Table 2), suggesting that the hydrophobic interaction may be one of the stabilizing factors of *Tt*PEPCK. The intraprotomer hydrogen-bonding interaction of *Tc*PEPCK has a greater ΔG value than those of other PEPCKs. This suggests that the intraprotomer hydrogen-bond interactions do not account for the thermostability of *Tt*PEPCK. Ion-pair networks on the protein surface are usually assumed to be a stabilizing factor (Hening *et al.*, 1995; Yip *et al.*, 1995; Pappenberger *et al.*, 1997). The total number of ion pairs (less than 3.4 Å) in the *Tt*PEPCK protomer is greater than those of other PEPCKs. The intraprotomer ion pairs might therefore contribute to the higher stability of *Tt*PEPCK. Entropic effects are also important stabilizing factors. When the conformational entropy of a protein is decreased in the denatured state, owing to substitutions or deletions, the protein may be stabilized. The denaturation entropies $-T\Delta S$ at 310.15 K for *Tt*PEPCK, *Tc*PEPCK and *Ec*PEPCK were calculated to be 486.9, 542.8 and 583.1 kJ mol^{-1}, respectively. This indicates that the entropic effects may contribute significantly to the higher stability of *Tt*PEPCK.

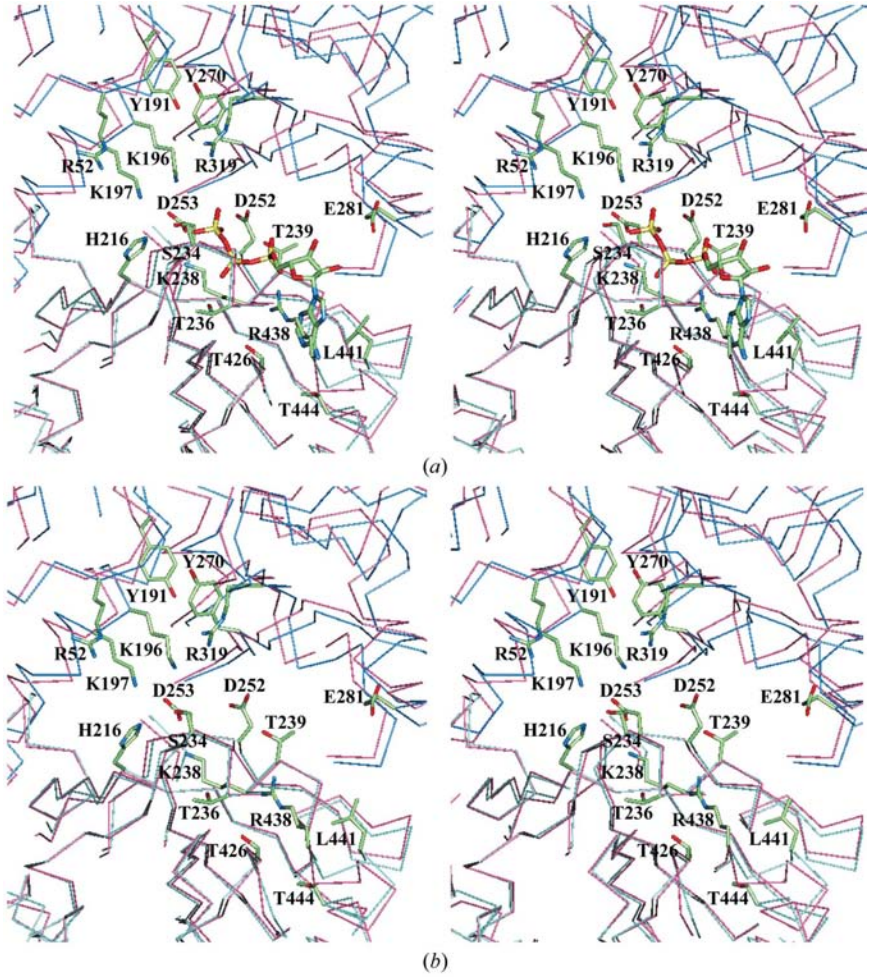

Figure 3
Stereoview of superimposed C$^{\alpha}$-trace models of closed (chain *A*) and open (chain *B*) protomers. The two chains are superimposed at the C-terminal domains to show the domain movement. The perspective and colouring of chain *A* are the same as those in Fig. 1. Chain *B* is coloured pink. The important conserved residues for catalysis are depicted as stick models on the C$^{\alpha}$-trace model of other residues. (*a*) Comparison of chains *A* and *B* in the ATP-liganded form. The bound ATP molecule is depicted as a stick model. (*b*) Comparison of chains *A* and *B* in the unliganded form.

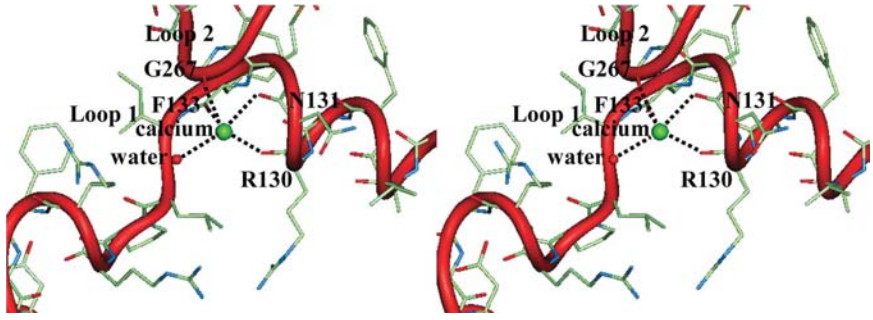

Figure 4
Stereo representation of the calcium-binding site. Bound calcium and water are depicted as green and red spheres, respectively.

The entropic effects are caused by the introduction of disulfide bonds, the side-chain substitution to Pro and the shortening of polypeptides. None of the three PEPCKs contain disulfide bonds. The numbers of Pro residues are 40, 26 and 27 in *Tt*PEPCK, *Tc*PEPCK and *Ec*PEPCK, respectively. Therefore, the greater number of Pro residues in *Tt*PEPCK contributes to the entropic effects.

*Tt*PEPCK with/without calcium was examined by differential scanning calorimetry (DSC) to detect differences in thermal behaviour. The T_m for *Tt*PEPCK in the presence of 0.5 m*M* calcium was 373.9 K. The T_m decreased to 372.4 K when *Tt*PEPCK was in the presence of 1 m*M* ethylenediaminetetraacetic acid (EDTA). Thus, the T_m of the *Tt*PEPCK increases only 1.5 K in the presence of calcium. From the reported DSC data, the T_m values of mutant human lysozyme (Kuroki *et al.*, 1992) and bovine recombinant α-lactalbumin (Veprintsev *et al.*, 1999) increase over 10 K upon binding calcium. The small ΔT_m value of 1.5 K for *Tt*PEPCK indicates a very weak association of calcium, which is not consistent with the observed tight coordination of calcium and the fact that no extra calcium was added to the crystallization setup of *Tt*PEPCK. The DSC results shows that the small ΔT_m value might arise from interactions at another minor calcium-binding site of *Tt*PEPCK. Unfortunately, a crystallographic identification of the minor site is currently impossible because the crystals of *Tt*PEPCK can be obtained only in the presence of high concentration of phosphate, which will disturb cocrystallization with calcium. In order to examine whether the bound calcium ion at the major site can be removed by treatment with 1 m*M* EDTA, the crystals were soaked into a stabilizing solution composed of 1 m*M* EDTA and 0.91 *M* potassium phosphate/1.3 *M* sodium phosphate pH 6.8 for up to 8 d. The soaked crystals showed no difference in the temperature factor of calcium at the major site, although no apparent steric hindrance from crystal packing is observed. These observations suggest that the bound calcium may substantially contribute to the thermostability of this enzyme. Interestingly, the major calcium site is located in the vicinity of the three interdomain hinge regions. The tightly bound calcium could stabilize the N-terminal domain structure and may be essential for the conformational transition of *Tt*PEPCK at high temperature. In conclusion, the higher stability of the protomer structure of *Tt*PEPCK might be provided from a combination of hydrophobic effects, ion pairs, entropic effects and the bound calcium.

Michi. S. solved the structure and wrote the paper, NO performed the enzymatic experiment, YU carried out the large-scale protein production, Mitsu. S. contributed to the automated crystallization and NK supervised this work. We thank K. Yutani for useful discussion on the DSC experiment, M. R. N. Murthy for critical reading of the manuscript and the beamline staff for assistance during data collection at BL26B1 and BL38B1 of SPring-8. The expression plasmid of *Tt*PEPCK (TT0460/HTPF00012) was supplied from the RIKEN Structurome Group, headed by S. Kuramitsu and S. Yokoyama. This work was supported by 'National Project on Protein Structural and Functional Analysis' funded by the MEXT of Japan.

References

Anderson, C. M., Zucker, F. H. & Steiz, T. A. (1979). *Science*, **204**, 375–380.

Berger, C., Weber-Bornhauser, S., Eggenberger, J., Hanes, J., Prückthun, A. & Bosshard, H. R. (1999). *FEBS Lett.* **450**, 149–153.

Britton, K. L., Baker, P. J., Borges, K. M., Engel, P. C., Pasquo, A., Rice, D. W., Robb, F. T., Scandurra, R., Satillman, T. J. & Yip, K. S. (1995). *Eur. J. Biochem.* **229**, 688–695.

Brünger, A. T., Adams, P. D., Clore, G. M., DeLano, W. L., Gros, P., Grosse-Kunstleve, R. W., Jiang, J.-S., Kuszewski, J., Nilges, M., Pannu, N. S., Read, R. J., Rice, L. M., Simonson, T. & Warren, G. L. (1998). *Acta Cryst.* D**54**, 905–921.

Chan, M. K., Mukund, S., Klezin, A., Adams, M. W. W. & Rees, D. C. (1995). *Science*, **267**, 1463–1469.

Connolly, M. L. (1993). *J. Mol. Graph.* **11**, 139–141.

Cymeryng, C., Cazzulo, J. J. & Cannata, J. J. B. (1995). *Mol. Biochem. Parasitol.* **73**, 91–101.

Delbaere, L. T. J., Sudom, A. M., Prasad, L., Leduc, Y. & Goldie, H. (2004). *Biochim. Biophys. Acta*, **1697**, 271–278.

Dunten, P., Belunis, C., Crowther, R., Hollfelder, K., Kammlott, U., Levin, W., Ramsey, M. G. B., Swain, A., Weber, D. & Wertheimer, S. J. (2002). *J. Mol. Biol.* **316**, 257–264.

Finnegan, P. M. & Burnell, J. N. (1995). *Plant Mol. Biol.* **27**, 365–376.

Funahashi, J., Takano, K., Yamagata, Y. & Yutani, K. (1999). *Protein Eng.* **12**, 841–850.

Hennig, M., Darimont, B., Sterner, R., Kirschner, K. & Jansonius, J. N. (1995). *Structure*, **3**, 1295–1306.

Hunt, M. & Köhler, P. (1995). *Biochim. Biophys. Acta*, **1249**, 15–22.

Kauzmann, W. (1959). *Adv. Protein Chem.* **14**, 1–63.

Korndorfer, I., Steipe, B., Huber, R., Tomschy, A. & Jaenicke, R. (1995). *J. Mol. Biol.* **246**, 511–521.

Koshland, D. E. (1958). *Proc. Natl Acad. Sci. USA*, **44**, 98–104.

Kunishima, N., Shimada, Y., Tsuji, Y., Sato, T., Yamamoto, M., Kumasaka, T., Nakanishi, S., Jingami, H. & Morikawa, K. (2000). *Nature (London)*, **407**, 971–977.

Kuroki, R., Kawakita, S., Nakamura, H. & Yutani, K. (1992). *Proc. Natl Acad. Sci. USA*, **89**, 6803–6807.

Laskowski, R. A., MacArthur, M. W., Moss, D. S. & Thornton, J. M. (1993). *J. Appl. Cryst.* **26**, 283–291.

Linss, J., Goldenberg, S., Urbinam, J. A. & Amazel, L. M. (1993). *Gene*, **136**, 69–77.

Matte, A., Goldie, H., Sweet, R. M. & Delbaere, L. T. J. (1996). *J. Mol. Biol.* **256**, 126–143.

Matte, A., Tari, L. W. & Delbaere, L. T. J. (1998). *Structure*, **6**, 413–419.

Matte, A., Tari, L. W., Goldie, H. & Delbaere, T. J. (1997). *J. Biol. Chem.* **272**, 8105–8108.

Navaza, J. (1994). *Acta Cryst.* A**50**, 157–163.

Oobatake, M. & Ooi, T. (1993). *Prog. Biophys. Mol. Biol.* **59**, 237–284.

Østerås, M., Driscoll, B. T. & Finan, T. M. (1995). *J. Bacteriol.* **177**, 1452–1460.

Otwinowski, Z. & Minor, W. (1997). *Methods Enzymol.* **276**, 307–326.

Pace, C. N., Vajdos, F., Fee, L., Grimsley, G. & Gray, T. (1995). *Protein Sci.* **4**, 2411–2423.

Pappenberger, G., Schuring, H. & Jaenicke, R. (1997). *J. Mol. Biol.* **274**, 676–683.

Russell, R. J. M., Hough, D. W., Danson, M. J. & Taylor, G. L. (1994). *Structure*, **2**, 1157–1167.

Schumann, J., Bohm, G., Schumacher, G., Rudolph, R. & Jaenicke, R. (1993). *Protein Sci.* **10**, 1612–1620.

Sudom, A., Walters, R., Pastushok, L., Goldie, D., Prasad, L., Delbaere, L. T. J. & Goldie, H. (2003). *J. Bacteriol.* **185**, 4233–4242.

Sugahara, M. & Miyano, M. (2002). *Tanpakushitsu Kakusan Koso*, **47**, 1026–1032.

Takano, K., Yamagata, Y., Funahashi, J., Hiroki, Y., Kuramitsu, S. & Yutani, K. (1999). *Biochemistry*, **38**, 12698–12708.
Tanaka, H., Chinami, M., Mizushima, T., Ogasawara, K., Ota, M., Tsukihara, T. & Yutani, K. (2001). *J. Biochem.* **130**, 107–118.
Tanner, J., Hecht, R. M. & Krause, K. L. (1996). *Biochemistry*, **35**, 2597–2609.
Tari, L. W., Matte, A., Goldie, H. & Delbaere, L. T. J. (1997). *Nature Struct. Biol.* **4**, 990–994.
Tari, L. W., Matte, A., Pugazhenthi, U., Goldie, H. & Delbaere, L. T. J. (1996). *Nature Struct. Biol.* **3**, 355–363.
Tortora, P., Hanozet, G. M. & Guerritore, A. (1985). *Anal. Biochem.* **144**, 179–185.
Trapani, S., Linss, J., Goldenberg, S., Fischer, H., Craievich, A. F. & Oliva, G. (2001). *J. Mol. Biol.* **313**, 1059–1072.
Urbina, J. A. (1987). *Arch. Biochem. Biophys.* **258**, 186–195.
Utter, M. F. & Kolenbrander, H. M. (1972). *The Enzymes*, 3rd ed., edited by P. D. Boyer, pp. 117-168. New York: Academic Press.
Valera, A., Pujol, A., Pelegrin, M. & Bosch, F. (1994). *Proc. Natl Acad. Sci. USA*, **91**, 9151–9154.
Veprintsev, D. B., Narayan, M., Permyakov, S. E., Uversky, V. N., Brooks, C. L., Cherskaya, A. M., Permyakov, E. A. & Berliner, L. J. (1999). *Proteins*, **37**, 65–72.
Yip, K. S. P., Stillman, T. J., Britton, K. L., Artymiuk, P. J., Sedelnikova, S. E., Engel, P. C., Pasquo, A., Chiaraluce, R. & Consalvi, V. (1995). *Structure*, **3**, 1147–1158.
Yokoyama, S., Hirota, H., Kigawa, T., Yabuki, T., Shirouzu, M., Terada, T., Ito, Y., Matsuo, Y., Kuroda, Y., Nishimura, Y., Kyogoku, Y., Miki, K., Masui, R. & Kuramitsu, S. (2000). *Nature Struct. Biol.* **7**, 943–945.
Yoshizaki, F. & Imahori, K. (1979). *Agric. Biol. Chem.* **43**, 397–399.